diffusion-fundamentals

The Open-Access Journal for the Basic Principles of Diffusion Theory, Experiment and Application

Diffusion-Ordered (DOSY) NMR of Solute Exchange Across the Human Erythrocyte Membrane: including an application of Post-Widder Laplace inversion

Bogdan E. Chapman and Philip W. Kuchel

School of Molecular and Microbial Biosciences, University of Sydney, NSW 2006 Australia

Corresponding author: P. W. Kuchel, School of Molecular and Microbial Biosciences, Building G08, University of Sydney, NSW 2006, Australia. E-mail: p.kuchel@mmb.usyd.edu.au

Abstract

Nuclear magnetic resonance (NMR) spectroscopy was used to study exchange of three distinctly different molecules across the membranes of human red blood cells (RBCs). In studying water, *t*-butanol, and dimethyl sulfoxide we exploited the marked differences in the apparent diffusion coefficients of these species inside and outside the cells in suspensions. The measurements were made with diffusion ordered spectroscopy (DOSY) with a domain of 'diffusion times' of 20 - 100 ms. In attempting to make the DOSY spectra quantitative we identified time domains for each of the three molecules in which the spectra showed well resolved peaks, and those in which only a single peak was evident for two of the species. The apparent mean resident times for water and *t*-butanol in the RBCs estimated by the methodology were ~17 ms, while the DMSO exchange was too slow, on the NMR timescale, to be quantified by this method. However, it is very clear that other methods that are based on regression analysis with a prescribed fitting function provide more reliable estimates of exchange rate constants. Also, to make the DOSY analysis more generally accessible we implemented a Laplace transform inversion method (the Post-Widder algorithm), and a procedure for enhancing the resolution of the resulting diffusion spectra by using standard functions in *Mathematica*.

Keywords

Membrane transport; red blood cell; inverse Laplace transform; dimethylsulfoxide; *t*-butanol; Post-Widder algorithm

Abbreviations

1D, one dimensional; 2D, two dimensional; DMSO, dimethyl sulfoxide; DOSY, diffusion ordered spectroscopy; PGSE, pulsed field-gradient spin-echo; RBC, red blood cell.

Introduction

The aim of this study was to investigate the use of the nuclear magnetic resonance (NMR) two dimensional (2D) diffusion-ordered spectroscopy (DOSY) experiment to measure exchange rates of solutes between the intra- and extracellular compartments of an erythrocyte (RBC) suspension. This method exploits the different apparent diffusion coefficients of the solutes in each compartment to distinguish between the exchanging populations.

A pulsed field-gradient spin-echo (PGSE) method for measuring the exchange rate constants of a solute or solvent in a two-compartment system has been described by Kärger et al. [1,2]. The method relies on the molecule having a different diffusion coefficient value in each compartment and the expression describing the attenuation of the NMR signal, R, is bi-exponential:

$$R = P_1 \exp(-KD_1\Delta) + P_2 \exp(-KD_2\Delta) \quad , \qquad (1)$$

where D_1, D_2, P_1 and P_2 are the apparent diffusion coefficients and population fractions, respectively, that are functions of the true parameters modulated by exchange, in each compartment. K is equal to $\gamma^2\delta^2g^2$ where γ is the magnetogyric ratio of the observed nucleus; δ is the gradient duration; g the gradient amplitude; and Δ is the time between the gradient pulses and defines the 'diffusion period or interval'. In subsequent analysis described in the Appendices we use $b = K\Delta$.

In a suspension of RBCs the cell membrane acts as a semi-permeable barrier to some molecules and since the intracellular milieu has a high protein concentration, this results in different diffusion coefficients for the molecules in the intra- and extracellular compartments. The molecules undergo restricted diffusion in the intracellular compartment and obstructed diffusion in the extracellular compartment. The technique has been used to measure quantitatively the exchange of water [3] and formate ions [4] across the membranes of intact RBCs.

DOSY [5] is a powerful technique to resolve the overlapping peaks in 1-dimensional (1D) spectra of components of a mixture of solutes, based on differences in their apparent diffusion coefficients. 2D-DOSY spectra are obtained by a suitable Laplace inversion of data from stacked plots of diffusion-attenuated 1D PGSE spectra that at each chemical shift are described by the sum of decaying exponentials. The result is a 2D spectrum with chemical shift on one axis and the distribution of diffusion coefficients on the other axis. Molecules with overlapping resonances are separated on the basis of their diffusion coefficients in this "diffusion dimension" [6]. A review of the technique is presented elsewhere [7].

The effects on DOSY spectra of protons on a molecule exchanging between two chemically distinct sites with different diffusion coefficients and the same chemical shift have been theoretically addressed by Johnson [8]; but to our knowledge no experimental data for a two-site *membrane transport* system have been presented. If the diffusion coefficients of the molecule in the two sites are sufficiently different, and provided that there is negligible exchange during the diffusion period, then two peaks at different diffusion coefficients should be seen in the DOSY spectrum. If any one molecule exchanges many times between the two sites during the diffusion period then a single peak at an intermediate diffusion coefficient should be seen in the DOSY spectrum.

Although the effect of two-site exchange on DOSY spectra has been analysed, there are few detailed reports of the use of the theory in the literature: The exchange of labile amide and hydroxyl protons with bulk water provides important information about the structures of biological molecules, as was shown in a study of the amide proton exchange rates, obtained from diffusion measurements, in the antibiotic peptide viomycin [9].

A DOSY study of the exchange of saccharose hydroxyl protons with bulk water in a water/d_6-DMSO solvent mixture has been presented [10]. Adjusting the solvent ratio allows control over the relative exchange rates of labile protons; hence the system may be placed experimentally into slow exchange with respect to chemical shift. Thus resonances at different chemical shifts are observed for bulk water and the various saccharose hydroxyl protons [10]. A series of DOSY spectra recorded at increasing diffusion times shows that as the diffusion time is increased the apparent diffusion coefficient of the labile hydroxyl protons approaches that of bulk water, with the more labile protons approaching most rapidly the diffusion coefficient of bulk water. This provides a *qualitative* estimate of the relative rates of exchange of the saccharose hydroxyl protons with water and the rates agree with quantitative measurements of exchange obtained from a 2D-EXSY experiment.

The exchange of the hydroxyl proton of *t*-butanol with bulk water in a water/d_6-DMSO solvent mixture has been reported [11]. The quantitative measurements of the hydroxyl exchange rate were determined by simulating the attenuation of the hydroxyl magnetization as a function of gradient strength during the PGSE experiment. The data are consistent with the apparent diffusion coefficients estimated from DOSY spectra.

The three previous studies were on systems where labile protons exchange between two different chemical environments that have different diffusion coefficients. An RBC suspension in contrast has two different *physical* environments, where a molecule that exchanges across the membrane experiences two different diffusion coefficients caused by restricted diffusion inside the cells and, to a lesser extent, obstructed diffusion when outside them. In general, the proton chemical shifts of a molecule are the same both inside and outside RBCs as there is little alteration of resonance frequency in the two chemical environments; however there are some solutes for which the different environments *do* produce an experimentally exploitable difference in frequency [12-14].

In this paper we present a DOSY study of the exchange of H_2O, and a mixture consisting of HOD, DMSO and *t*-butanol across the membranes of intact RBCs. High concentrations of DMSO and *t*-butanol were introduced into RBCs without deleterious effects on them, and the three molecules had different transmembrane exchange rates. However, quantitative estimates of the exchange rate constants, other than order-of-magnitude estimates were not able to be made in contradistinction to other methods that involve direct-regression of a predetermined fitting function [e.g., 15] .

Materials and Methods

Sample Preparation

All chemicals were of Analytical Reagent (AR) grade. Dimethylsulfoxide (DMSO) was obtained from Sigma (St. Louis, MO, USA) and *t*-butanol was from Ajax Chemicals (Seven Hills, NSW, Australia). D_2O was obtained from ANSTO (Lucas Heights, NSW, Australia).

Freshly drawn venous blood was washed twice in ice cold H_2O/saline (154 mM NaCl, 5 mM glucose). Following centrifugation at 3000 x g at 4^{o}C the plasma and white-cell buffy coat were removed by aspiration using a water pump. The washed RBCs were suspended in saline solution and bubbled with CO for ~5 min to convert oxy- and deoxyhaemoglobin to diamagnetic carbonmonoxyhaemoglobin; the CO results in improved spectral resolution [12]. RBCs used for studies on the exchange of H_2O were washed once more in H_2O/saline. When the exchange of HOD, DMSO, and *t*-butanol were studied the RBCs were washed further with D_2O/saline/5 mM glucose, and three more times in the same buffer containing increasing amounts of dimethylsulfoxide (DMSO) and *t*-butanol; the concentration of the two solutes had to be gradually increased otherwise the cells lysed. The final concentrations of DMSO and *t*-butanol were 230 and 106 mM, respectively, giving methyl group proton

concentrations of 1380 and 954 mM for the two solutes. Washing the cells in D_2O reduced the size of the ^1H_2O signal to approximately the same size as those from the other two solutes. The HOD concentration was estimated, from integral ratios, to be ~1100 mM. Samples of 1 cm length were made up to a haematocrit of 0.7 in 5-mm outer-diameter Shigemi NMR tubes (Wilmad, Buena, NJ, USA).

NMR spectroscopy

NMR spectra were obtained on a Bruker (Karlsruhe, Germany) DRX-400 spectrometer with a 9.4 T vertical wide-bore magnet operating at 400.13 MHz for ^1H observation. A Bruker Diff-25 diffusion probe capable of providing gradients of up to 9800 mT m^{-1} in the z-direction was used. The gradient generated in this probe is linear over 1 cm. The experiments were run unlocked as this probe does not have a deuterium lock channel; this diminished the quality of the DOSY spectra as any field drift altered the resonance frequency of the peaks during the measurement, adversely affecting the Laplace transform in the second dimension of the 2D spectrum. Experiments were conducted at 25°C and were of approximately 40 min duration.

A bipolar longitudinal eddy current delay (BPLED) pulse sequence [16] was used to obtain DOSY spectra. Sine-shaped gradients of 1 ms duration ($\delta/2$) were used in all experiments with a delay, τ, the time between the bipolar gradients, of 5 ms. DOSY spectra were acquired at various diffusion times, Δ, the time between the leading edges of the encoding and decoding gradients. For each experiment 32 spectra were obtained with the gradient strength varied in equal increments. The gradient was varied, for an H_2O washed sample, from 50 mT m^{-1} to a maximum of 1960 mT m^{-1} (for Δ = 20 ms) to attenuate the ^1H_2O signal to <5% of its initial intensity. For larger values of Δ the maximum gradient required to attenuate the signal was less. For an HOD, DMSO, *t*-butanol washed sample a maximum gradient of 3450 mT m^{-1} (Δ = 20 ms) was required to attenuate the intracellular DMSO peak to <5% of its original intensity. Typically, 16 transients were acquired into 4k data points using a spectral width of 4000 Hz. The spectra were processed using an exponential apodization function corresponding to a 3 Hz line broadening and Fourier transformed into 8k data-point spectra. DOSY spectra were processed with the Bruker XWINNMR software package using a two-exponential fit to the data.

Numerical analysis

Nonlinear regression analysis of the primary PGSE data was carried out by using Origin Pro software (OriginLab, Northampton, MA, USA); standard errors and residuals were generates by the fitting routines.

Results and Discussion

DOSY of ^1H_2O in RBCs

Figure 1 shows DOSY spectra of an H_2O/saline washed RBC suspension recorded at three diffusion times, Δ = 20, 60, and 140 ms. With increasing diffusion time the two peaks evident with Δ = 20 ms (Fig. 1A), coalesced to leave only one when Δ = 140 ms (Fig. 1C) thus yielding a single average diffusion coefficient value. The mean residence time of a water molecule in an RBC is ~13 ms at 25°C [17], so a water molecule would have exchanged ~11 times between the intra- and extra-cellular compartments when Δ = 140 ms. This time corresponded to that in which coalescence of the two peaks was observed. Calculations by Johnson [8] show that for a two-site exchange system with equal mean residence times for the spins at each site, more than six exchanges between sites must occur during the diffusion

time to observe a single average diffusion coefficient. Therefore for the RBC suspensions estimates of the mean lifetime of water could be made (see below).

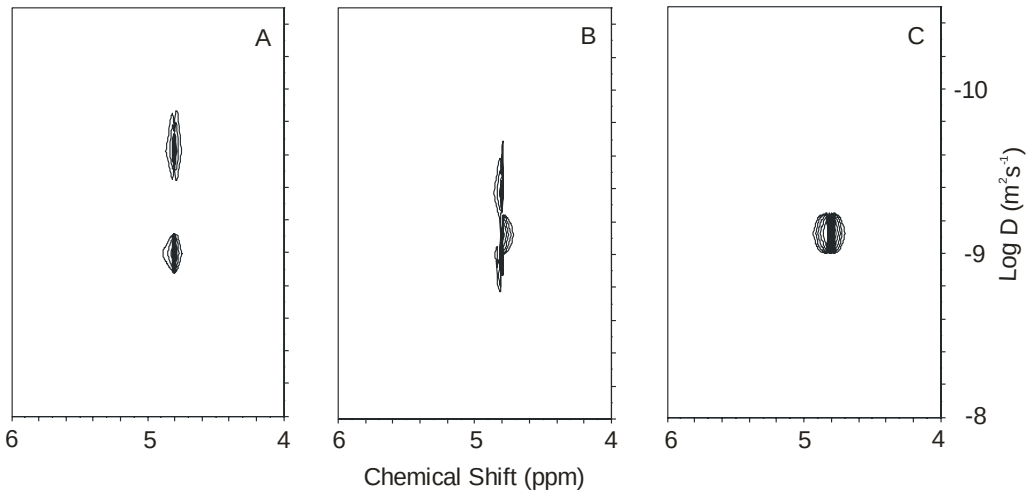

Fig.1: Contour-plot DOSY ^{1}H NMR spectrum of RBCs washed in H_2O/saline. The values of the diffusion time Δ were 20 ms (A), 60 ms (B) and 140 ms (C). Experimental conditions and NMR parameters are given in Materials and Methods.

DOSY of HOD, DMSO and *t*-butanol in RBCs

The equilibrium ^{1}H NMR spectrum of a suspension of RBCs that has been washed in D_2O/saline, DMSO and *t*-butanol is shown in Fig.2. HOD and *t*-butanol exchanged across the RBC membrane on the millisecond timescale and DMSO exchange was on the tens-of-seconds time scale. Thus the DMSO molecules were effectively trapped in the intra- and extra-cellular compartments during the relatively short diffusion times used in these experiments. Intra- and extracellular HOD and *t*-butanol have resonances with the same chemical shift in both compartments respectively. The peak from DMSO showed a small "split peak" effect usually seen in ^{31}P and ^{19}F spectra of phosphorous [18] and fluorine containing compounds [19] that exchange across the RBC membrane. The peak separation between signals from intra- and extracellular DMSO was 12 Hz and extracellular DMSO gave rise to the high frequency peak.

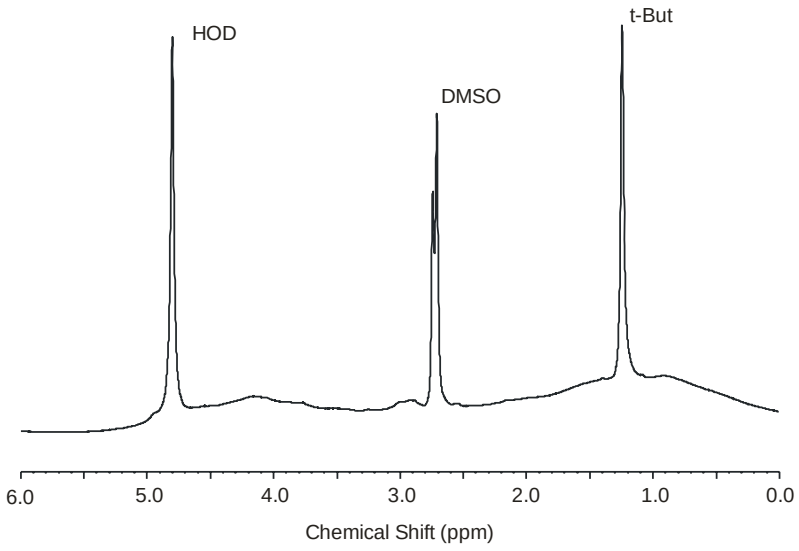

Fig. 2: ^{1}H NMR spectrum of a suspension of RBCs, haematocrit 0.7, washed with D_2O/saline containing 106 mM *t*-butanol and 230 mM DMSO. Experimental conditions and NMR parameters are given in Materials and Methods.

Figure 3 shows DOSY spectra of RBCs washed in D_2O/saline containing DMSO and *t*-butanol, recorded with three different diffusion times: at Δ = 100 ms the HOD and *t*-butanol signals showed a single average diffusion coefficient for the intra- and extra-cellular compartments. This was the outcome expected for rapidly exchanging molecules.

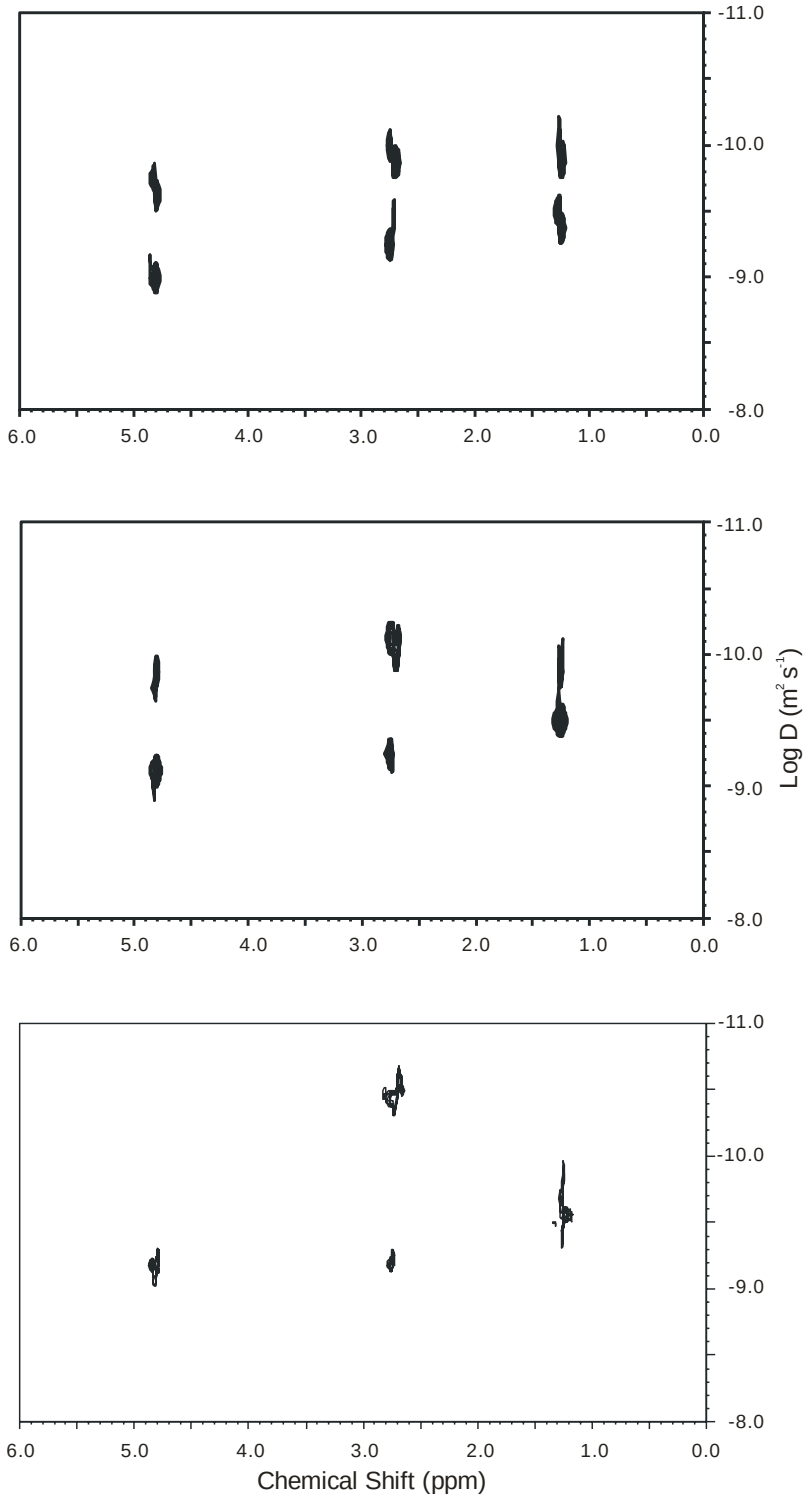

Fig. 3: Contour-plot DOSY ^{1}H NMR spectra of RBCs washed in D_2O/saline containing 106 mM *t*-butanol and 230 mM DMSO. The values of the diffusion time, Δ, were 20 ms (**A**), 40 ms (**B**) and 100 ms (**C**). Details of the experimental conditions and NMR measurements are given in Materials and Methods.

A value of ~17 ms was deduced for the mean residence time of water and *t*-butanol using Johnson's calculation (7) that, for a two-site exchange system, six exchanges of the spin between sites must occur during the diffusion time to observe a single, average, diffusion coefficient. The diffusion coefficient of the intracellular DMSO signal however showed the effect of restricted diffusion when the measured value became smaller at longer diffusion times [20]. Molecules that are effectively trapped inside or outside RBCs during the diffusion time are expected to give a separate peak in the DOSY spectrum.

The estimated extra-cellular DMSO diffusion coefficient was relatively unaffected by the range of diffusion times used for the measurements. This is consistent with DMSO undergoing relatively unrestricted diffusion in the space outside the RBCs.

Laplace inversion in DOSY

The utility of DOSY to provide a distribution of diffusion coefficients for the construction of 2D displays depends on taking the inverse Laplace transform of intensities from stacked plots of diffusion-attenuated spectra. However, the technique is beset with computational difficulties: Analysis using the Bruker XWINNMR software involves selecting a global one-, two- or three-component exponential fit to the diffusion data and then Laplace-inverting the exponential decays obtained from the regression analysis. Fitting a function that is the sum of two exponentials to a decay curve that is actually a single exponential can result in fitting the second exponential with a very small amplitude, or two exponentials are fitted with very similar apparent diffusion coefficients. In view of these problems the experimentalist is required to specify the number of exponentials in the fitted function; and this function is then used in all subsequent data columns of the spectral set. This blanket specification of a general fitting function for all peaks may not be appropriate. On the other hand in methods such as SPLMOD [7] the program automatically attempts fitting one-, two- or three-exponential fits to each column of data, and it determines which of the fits is statistically the "best". The number of exponentials that gives the best fit is evaluated individually for each column of data.

The DOSY spectrum for H_2O in an RBC suspension at a diffusion time of Δ = 20 ms (Fig. 1A) yielded two apparent diffusion coefficients of 2.2 x 10^{-10} m^2 s^{-1} and 9.1 x 10^{-10} m^2 s^{-1}. The integrals of the diffusion-attenuated water signal from this experiment were also fitted to a two-exponential decay model using the program Origin. Namely,

$$R(b) = P_1(0)\, e^{-D_1 b} + P_2(0)\, e^{-D_2 b} \quad , \qquad (2)$$

where $P_1(0) = 0.275$, $P_2(0) = 0.725$, $D_1 = 2.42 \times 10^{-10}$, $D_2 = 10.67 \times 10^{-10}$. Values of 2.4 x 10^{-10} m^2 s^{-1} and 10.7 x 10^{-10} m^2 s^{-1} were obtained. It can be seen that these values are in very good agreement with those obtained by the inverse Laplace transformation used to obtain the DOSY spectra.

Alternative Laplace inversion

Since the inception of DOSY, with its use of the CONTIN [22] algorithm, other methods of Laplace inversion of NMR-diffusion data have not been widely used. The method exists in a mature and apparently optimized form. However, there is merit in having to hand an algorithm that is very easily implemented and for which the various stages of its application are open to ready graphical inspection. Such a direct numerical method was used previously to obtain "kinetic" spectra from superimposed NMR peaks of different relaxation times in RBC suspensions [21]. The method is the real inversion formula of Post and Widder [23,24]. Since the algorithm appears not to have been previously applied to NMR-diffusion data, we explored its strengths and weaknesses in analyzing PGSE data from the sample of ^1H_2O in RBCs used to generate Fig. 1A.

We focus attention here on the data analysis that began with the series of PGSE spectra used to generate Fig. 1A which are shown in the inset of Fig. 4. Even allowing for the small size of this figure it is impossible to perceive if there are single- or double-exponential features of the dependence of PGSE signal intensity on the value of *b*. The graph of these data, interpolated by a shifting cubic spline, versus Ln(*b*) are clearly sigmoidal (Fig. 4).

The mathematical details of the Post-Widder algorithm, as it applies to PGSE data are given in Appendix 1; and an implementation in *Mathematica* [24] is given in Appendix 2.

The analysis simply requires the generation of a plot of the second derivative of the Stejskal-Tanner data minus the first derivative [Eq. (A9)] versus Ln(2) – Ln(*b*). The plot gave the distribution function of the values of *D* and the abscissal positions of the maxima gave the estimates of the mean apparent diffusion coefficients.

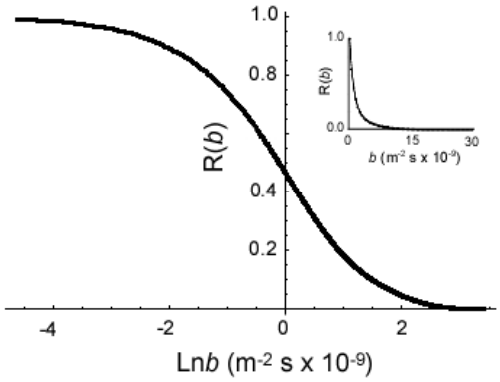

Figure. 4: ^{1}H NMR PGSE data from Fig. 1A of $^{1}H_2O$ diffusion in a suspension of RBCs obtained with Δ = 20 ms and δ = 2 ms. The inset shows the plot of Eq. (1) onto the primary PGSE data with the fitted parameters that are given below Eq. (2). The main graph of the figure shows the same smooth data, with an interpolation function applied, plotted versus Ln*b*. This processing of the data was a prelude to applying the Post-Widder algorithm for Laplace inversion of the data.

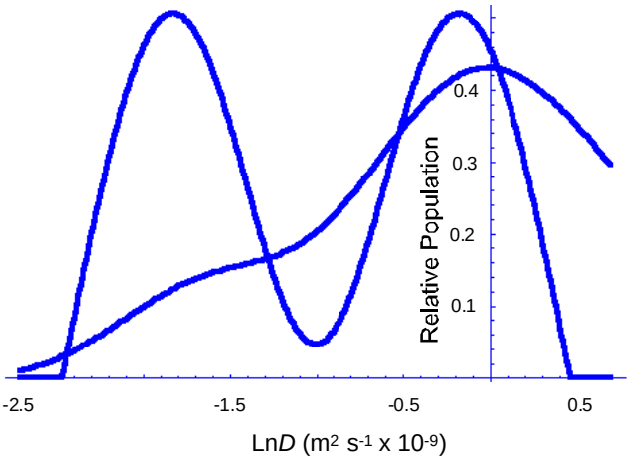

Figure 5: Graph of the calculated *D*-distribution (the lower curve) and the *D*-distribution with enhanced-resolution (the curve with two peaks of similar amplitude). The position of the maxima in the un-enhanced plot corresponded to values of 2.2 x 10^{-10} m^2 s^{-1} and 10.0 x 10^{-10} m^2 s^{-1}, in excellent agreement with the values used to generate Fig. 4 in the first place. The resolution-enhanced maxima are shifted to the left but give values of D that are similar the previous values.

The position of the maxima in the un-enhanced Post-Widder plot in Fig. 5 gave values of 2.2 x 10^{-10} m^2 s^{-1} and 10.0 x 10^{-10} m^2 s^{-1} that are in excellent agreement with the values that were used to generate the curve in Fig. 4 in the first place, and with the DOSY-derived values of 2.2 x 10^{-10} m^2 s^{-1} and 9.1 x 10^{-10} m^2 s^{-1}.

The Laplace transform of e^{-Db}, where *b* is the independent variable, is $1/(s + D)$ [26]; and when this function is plotted as an absolute value versus the Laplace variable, *s*, it gives a peak with a singularity at $s = -D$ and 'wings' like that of a Lorentzian spectral line. The Post-Widder algorithm correctly gives a single peak centred on *D* for the transformation of an exponential function. However, it generates a peak that is much wider than the analytical inverse. When there are two exponentials, as shown in Fig. 5, this broadening becomes a barrier to precise identification of the maxima, and hence estimates of the diffusion coefficients. Therefore an additional step in the analysis can be to sharpen the rather broad peaks in the Post-Widder diffusion spectra by applying a type of signal enhancement. The simplest approach is via the convolution theorem of Fourier analysis [27]. Our implementation in *Mathematica* of this signal enhancement is given in Appendix 2. And the resolution-enhanced diffusion spectrum shown in Fig. 5 is a curve in which the maxima are shifted to the left; but the implied values of D are the close to the previous ones.

It will not have escaped the reader's attention that all we seem to have achieved is another way of presenting the data that were analysed by nonlinear regression of a double exponential

onto the PGSE data. By doing this we obtained estimates of the two apparent *D* values for water inside and outside the RBCs. On the other hand this representation is the very basis of the DOSY analysis and as such the Post-Widder algorithm has been shown to be suitable for generating DOSY spectra. Certainly, the algorithm faithfully returned the values of the two diffusion coefficients that were used to represent the original data.

Conclusions

Our system of RBCs with three different molecular species, that exchanged across the human RBC membrane at different rates, showed characteristic DOSY spectra that were of comparable quality to those obtained with isotropic chemical solutions. However, the DOSY analysis did not yield estimates of diffusion coefficients that were sufficiently accurate or reproducible to enable application of the Kärger two-site exchange theory [1,2]; but more importantly the relative population sizes that are critical to exchange analysis could not be relied upon. The Kärger two-site analysis had been done previously by direct regression of the requisite function onto 1D PGSE data; and yet the DOSY representation of the data did provide a useful, visually evocative, indication that exchange was occurring across the RBC membranes. And we were able to estimate an order-of-magnitude value for the mean residence time of both water and *t*-butanol in the RBCs. The exchange rate of DMSO was substantially too slow for an estimate of the exchange rate to be made; the persistence of two peaks in the DOSY spectra for all the values of Δ is evidence of this (Fig. 3).

The Post-Widder algorithm for carrying out Laplace inversion of PGSE data was readily implemented in *Mathematica*, and presumably will be for similar high level programming packages. With a test function derived from the real data used for the DOSY analysis, the Post-Widder algorithm faithfully represented distributions of *D* values that had maxima at the values expected for the direct two-exponential fit to the primary data.

Finally, DOSY analysis provided a useful visual representation of the membrane transport system in RBC suspensions and yet quantification requires other well-established forms of data analysis. Given the conclusion that DOSY could only be used non-quantitatively, the Post-Widder algorithm provides a readily accessible means of generating the second dimension of 2D PGSE spectra.

Acknowledgments

The work as funded by a Discovery grant from the Australian Research Council. We thank Dr Bill Bubb and Mr Bill Lowe for expert NMR and technical assistance, respectively. Copies of the *Mathematica* programs used for this paper are available from PWK.

References

1. J. Kärger, H. Pfeifer, W. Heink, Principles and application of self-diffusion measurements by nuclear magnetic resonance. Adv. Magn. Reson. 12 (1988) 1-89.

2. A. R. Waldeck, P. W. Kuchel, A. J. Lennon, B. E. Chapman, NMR diffusion measurements to characterise membrane transport and solute binding. Progr. NMR Spectrosc. 30 (1997) 39-68.

3. J. Andrasko, Water diffusion permeability of human erythrocytes studied by a pulsed gradient NMR technique. Biochim. Biophys. Acta 428 (1976) 304-311.

4. U. Himmelreich, B.E. Chapman, P.W. Kuchel, Membrane permeability of formate in human erythrocytes: NMR measurements. Eur. Biophys. J. 28 (1999) 158-165.

5. K.F. Morris, C.S. Johnson, Jr., Diffusion-ordered two-dimensional nuclear magnetic resonance spectroscopy. J. Am. Chem. Soc. 114 (1992) 3139-3141.

6. A. Jershow, N. Müller, Diffusion-separated nuclear magnetic resonance spectroscopy of polymer mixtures. Macromolecules 31 (1998) 6573-6578.

7. C.S. Johnson, Jr., Diffusion ordered nuclear magnetic resonance spectroscopy: principles and applications. Prog. Nucl. Magn. Reson. Spectrosc. 34 (1999) 203-256.

8. C.S. Johnson, Jr., Effects of chemical exchange in diffusion-ordered 2D NMR spectra. J. Magn. Reson. A 102 (1993) 214-218.

9. M. Liu, H.C. Toms, G.E. Hawkes, J.K. Nicholson, J.C. Lindon, Determination of the relative NH proton lifetimes of the peptide analogue viomycin in aqueous solution by NMR-based diffusion measurement. J. Biomol. NMR **13** (1999) 25-30.

10. E.J. Cabrita, S. Berger, HR-DOSY as a new tool for the study of chemical exchange phenomena. Magn. Reson. Chem. 40 (2002) S122-S127.

11. E.J. Cabrita, S. Berger, P. Bräuer, J. Kärger, High-Resolution DOSY NMR with spins in different chemical surroundings: influence of particle exchange. J. Magn. Reson. 157 (2002) 124-131.

12. K. Kirk, P.W. Kuchel, The contribution of magnetic susceptibility effects to transmembrane chemical shift differences in the ^{31}P NMR spectra of oxygenated erythrocyte suspensions. J. Biol. Chem. 263 (1988) 130-134.

13. D. J. Philp, W. A. Bubb, P. W. Kuchel, Chemical shift and magnetic susceptibility contributions to the separation of intracellular and supernatant resonances in variable angle spinning NMR spectra of erythrocyte suspensions. Magn. Reson. Med. 51 (2004) 441-444.

14. T. J. Larkin, W. A. Bubb, P. W. Kuchel, pH and cell volume effects on H_2O and phosphoryl resonance splitting in rapid-spinning NMR of red cells. Biophys. J. (2006) in press.

15. K. P. Whittall, A. L. MacKay, Quantitative interpretation of NMR relaxation data. J. Magn. Reson. 84 (1989) 134-152.

16. D. Wu, A. Chen, C.S. Johnson, Jr., An improved diffusion-ordered spectroscopy experiment incorporating bipolar-gradient pulses. J. Magn. Reson. A 115 (1995) 260-264.

17. G. Benga, B.E. Chapman, C.H. Gallagher, D. Cooper, P.W. Kuchel, NMR studies of diffusional water permeability of red blood cells from macropodid marsupials (kangaroos and wallabies). Comp. Biochem. Physiol. 104A (1993) 799-803.

18. K. Kirk, P.W. Kuchel, Characterization of transmembrane chemical shift differences in the ^{31}P NMR spectra of various phosphoryl compounds added to erythrocyte suspensions. Biochemistry 27 (1988) 8795-8802.

19. A.S.L. Xu, J.R. Potts, P.W. Kuchel, The phenomenon of separate intra- and extracellular resonances of difluorophosphate in ^{31}P and ^{19}F NMR spectra of erythrocytes. Magn. Reson. Med. 18 (1991)193-198.

20. P.T. Callaghan, K.W. Jolley, R.S. Humphrey, Diffusion of fat and water in cheese as studied by pulsed field gradient nuclear magnetic resonance. J. Colloid Interface Sci. 93 (1983) 521-529.

21. B.T. Bulliman, P.W. Kuchel, Formation of "kinetic" spectra from superimposed NMR resonances of different relaxation times. J. Magn. Reson. 62 (1985) 556-560.

22. S.W. Provencher, R.H. Vogel, Numerical Treatment of Inverse Problems in Differential and Integral Equations, Birkhauser, Boston (1983).

23. D.V. Widder, The Laplace Transform, Princeton University Press, New Jersey (1941).

24. D.L. Olson, M.S. Shuman, Kinetic spectrum method for analysis of simultaneous, first-order reactions and application to copper(II) dissociation from aquatic macromolecules. Anal. Chem. 55 (1983) 1103-1107.

25. S. Wolfram, The Mathematica Book, 5th edn, Wolfram Media, Inc. (2003).

26. M.R. Spiegel, Theory and Problems of Laplace Transforms, McGraw-Hill, New York (1965).

27. M.R. Spiegel, Theory and Problems of Fourier Analysis, McGraw-Hill, New York (1974).

Appendix 1 Simple numerical Laplace inversion of PGSE data

In the PGSE experiment the spectral envelope of NMR resonances (peaks) of components with different diffusion coefficients in a mixture, for a given diffusion time, decreases with increasing magnetic field gradient strength. The two-site case is given by Eq. (1) but the general case of n sites is:

$$\mathrm{R}(b) = \sum_{i=1}^{n} \mathrm{P}_i(0)\, e^{-D_i b} \qquad \text{(A1)}$$

where b is the Stejskal-Tanner parameter, and $\mathrm{P}_i(0)$ is the proportion of the original signal assigned to each species-population that has a diffusion coefficient D_i, when $b = 0$. If the diffusion coefficient is considered to be the variable of integration then the sum in Eq. (A1) can be replaced by,

$$\mathrm{R}(b) = \int_0^\infty \mathrm{F}(D)\, e^{-Db} dD \quad . \tag{A2}$$

In this form R(b) is seen to be the Laplace transform of F(D) [26]; and F(D) is a distribution function of the values of D.
Hence,

$$\mathrm{R}(b) = \Im\{\mathrm{F}(D)\} \quad , \tag{A3}$$

where $\Im$ denotes the Laplace transform, and the distribution of the values of the diffusion coefficient is given by the inverse Laplace transform ($\Im^{-1}$) of R(b):

$$\mathrm{F}(D) = \Im^{-1}\{\mathrm{R}(b)\} \quad . \tag{A4}$$

It is the form of F(D) that we seek from the Laplace-inversion of the data R(b). Inversion is carried out in modern versions of DOSY with the sophisticated algorithm constructed by Provencher [22]. However, we show here that a much simpler and hence more transparent method can be used, at least to guide the use of more elaborate methods. The simple approach has the advantage of allowing manipulation and graphing of data that are transformed, at various stages of the analysis. It also has the advantage of using standard functions in the well known computing environment, *Mathematica* [25]. Specifically, the Post-Widder inversion formula on the real axis [23,24] and written in PGSE-NMR notation is:

$$\mathrm{F}(D) = \lim_{m\to\infty} \left(\frac{-1^m}{m!}\right)\left(\frac{m}{D}\right)^{m+1} \frac{\partial \mathrm{R}(m/D)}{\partial b^m} = \lim_{m\to\infty} \mathrm{F}_m(D) \tag{A5}$$

where m is a dummy-variable integer. The nomenclature m/D is used to indicate that b corresponds to this ratio, for any computed value of F(D). It is assumed that the approximation in Eq. (A5) improves as m increases and yet as this occurs increasingly higher order derivatives are required. It transpires that a choice of m = 2 is a practical compromise between a low order approximation and the noise introduced in taking higher numerical derivative of PGSE data. Hence the second order approximation with m = 2 in Eq. (A2) yields

$$\begin{aligned} \mathrm{R}(b) \; ; \;\; & \int_0^\infty \mathrm{F}_2(D)\, e^{-Db} dD \\ & \\ & = \int_0^\infty \left(\frac{4}{D^3}\right) \frac{\partial^2 \mathrm{R}(b)}{\partial b^2}\, e^{-Db} dD \end{aligned} \quad , \tag{A6}$$

Equation [A6] can be written as

$$\mathrm{R}(b) \; ; \;\; \int_0^\infty \left(\frac{4}{D^3 b^2}\right) \mathrm{H}(D,b)\, e^{-Db} dD \quad , \tag{A7}$$

where

$$\mathrm{H}(D,b) = b^2 \frac{\partial^2 \mathrm{R}(D,b)}{\partial b^2} \quad . \tag{A8}$$

Note that R is written as a function of both b and D, as seen from Eq. (A1), to give explicit meaning to the appearance of D on the left hand side of Eq. (A8). By using the change of variable $\partial \mathrm{L\,n}(b) = \frac{1}{b}\,\partial b$ in Eq. (A8) we obtain,

$$\begin{aligned} \mathrm{H}(D,b) &= b\,\frac{\partial}{\partial \mathrm{L\,n}(b)}\left[\frac{1}{b}\,\frac{\partial \mathrm{R}(D,b)}{\partial \mathrm{L\,n}(b)}\right] \\ &= \frac{\partial^2 \mathrm{R}(D,b)}{\partial [\mathrm{L\,n}(b)]^2} - \frac{\partial \mathrm{R}(D,b)}{\partial \mathrm{L\,n}(b)} \end{aligned} \quad , \tag{A9}$$

This is the key equation to which we return below. But it is useful to detour and consider that by differentiating Eq. (A1), Eq. (A9) gives,

$$\mathrm{H}(D,b) = \sum_{i=1}^{n} \mathrm{P}_i(0)\, D_i^2 b^2 e^{-D_i b} \quad . \tag{A10}$$

The integral of the distribution function should be the sum of the components for each diffusion coefficient, when $b = 0$. This is shown as follows from Eq. (A10):

$$\int_{-\infty}^{\infty} \mathrm{H}(D,b)\; d\mathrm{L\,n}(D) = \sum_{i=1}^{n} \mathrm{P}_i(0) \int_{-\infty}^{\infty} D^2\; b^2 e^{-Db}\, d\mathrm{L\,n}(D)\,, \tag{A11}$$

and the integral on the right-hand side of the equation is seen to have a simple solution, by noting that the Laplace transform of D is $1/b^2$,

$$\begin{aligned} \int_{-\infty}^{\infty} D^2 b^2 e^{-Db}\, d\mathrm{L\,n}(D) &= b^2 \int_{-\infty}^{\infty} D\; e^{-Db}\, dD \\ &= 1 \end{aligned} \quad . \tag{A12}$$

Therefore Eq. (A11) reduces to,

$$\int_{-\infty}^{\infty} \mathrm{H}(D,b)\; d\mathrm{L\,n}(D) = \sum_{i=1}^{n} \mathrm{P}_i(0)\,, \tag{A13}$$

which was sought. Also, note the interesting result that Eq. (A11) is symmetrical in D and b so,

$$\frac{\partial \mathrm{H}(D,b)}{\partial \mathrm{L\,n}\, D} = \frac{\partial \mathrm{H}(D,b)}{\partial \mathrm{L\,n}\, b}\,, \tag{A14}$$

and from Eq. (A11),

$$\int_{-\infty}^{\infty} H(D,b)\; d\mathrm{L}\,n(D) = \int_{-\infty}^{\infty} H(D,b)\; d\mathrm{L}\,n(b) = \sum_{i=1}^{n} P_i(0)\,. \qquad \text{(A15)}$$

And the distribution equation is seen to be the same whether it is plotted versus Ln(D) or Ln(b); but notably only Ln(b) is available to us from the experiments.

Returning to Eq. (A9), we note that b corresponds to (m = 2)/D so Ln(D) = Ln(2/b) = Ln(2) – Ln(b). Hence, a plot of the second derivative of the Stejskal-Tanner data minus the first derivative [Eq. (A9)] versus Ln(2) – Ln(b) gives the distribution function of the values of D.

Appendix 2 *Mathematica* implementation of Post-Widder Laplace inversion

To implement the above procedure, PGSE data are listed as (b, R(b)) pairs where R, the peak attenuation, is the spin-echo peak intensity normalized to the signal when the magnetic field gradients are zero. And b is the Stejskal-Tanner parameter, $b = \gamma^2 g^2 \delta^2 (\Delta - \delta/3)$, where the parameters are defined in the main text. The data are denoted by

```
data = {{b1, R(b1)},{ b2, R(b2},…};
(* Find the number of data pairs.*)
len1 = Length[data];
(* Convert the data so that b is replaced by Ln(b).*)
dataLn = Table[{Log[data[[j,1]], data[[j,2]]}, {j, 1, len1}];
(* Find the maximum value of Ln(b) in the data.*)
maxLnb = dataLn[[len1,1]];
(* Graph R versus Ln(b) data.*)
graph1= ListPlot[dataLn, PlotJoined -> True];
(* Interpolate a shifting cubic spine on the R versus Ln(b) data.*)
intDataLn = Interpolation[dataLn];
(* Obtain the zeroth, first and second derivatives of the interpolation function, where the
evaluation interval is chosen to be 0.02; but it could be any value depending on the
numerical resolution required.*)
intDataLnD0 = Table[{x, intDataLn[x]},{x, 0.001, maxLnb, 0.02}];
intDataLnD1 = Table[{x, intDataLn'[x]},{x, 0.001, maxLnb, 0.02}];
intDataLnD2 = Table[{x, intDataLn''[x]},{x, 0.001, maxLnb, 0.02}];
(* Obtain the length of the data file.*)
len2 = Length[intDataLnD2];
(* Change the abscissa as in the text below Eq. [A15] and, according to Eq. [A9], subtract
the first- from the second-derivative.*)
result = Table[{Log[2.0]- intDataLnD2[[j,1]], intDataLnD2[[j,2]] – intDataLnD1[[j,2]]},{j,1,
len2}];
graph2 = ListPlot[result, PlotJoined->True];

(* graph2 has the D-distribution plot, and the number of maxima indicate the number of
different species with the same resonance frequency while the maximum values give the
corresponding D values. *)
```

It is quite common that the D-distribution plot is not well resolved and resolution enhancement is sought. One way this can be implemented is by taking the Fourier transform

of the data, after first interpolating a shifting cubic-spline through it. The real part of the Fourier transformed data is multiplied by an increasing exponential prior to taking the inverse Fourier transform of the combined modified real and imaginary parts. An implementation of this in *Mathematica* is as follows.

```
len3  = Length[result];
minAbscissa = result[[len3,1]];
maxAbscissa = result[[1,1]];
interRes = Interpolation[result];
(* The list data2 contains the interpolation version of the D-distribution function. *)
data2 = Table[{x, interRes[x]}, {x, minAbscissa, maxAbscissa, 0.01}];
(* data3 contains just the interpolated  ordinate values of the D-distribution function. *)
data3 = Table[interRes[x], {x, minAbscissa, maxAbscissa, 0.01}];
(* Fourier transform data3. *)
fourierDist = Fourier[data3];
(* To inspect the real and imaginary parts of the Fourier transformed data execute the
following functions. *)
graph3 = ListPlot[Re[fourierDist], PlotJoined->True];
graph4 = ListPlot[Im[fourierDist], PlotJoined->True];
(* To apply resolution enhancement to the data multiply by an increasing (enhancing)
exponential and then take the inverse Fourier transform. The exponential 'rate constant' is
denoted kenh. *)
len4 = Length[fourierDist];
kenh = 2.5;
enhancRe = Table[Re[fourierDist[[j]]] e^(kenh*j/len4), {j, 1, len4}];
enhancTot = Table[{enhancRe [[j]] + Im[fourierDist[[j]]}, {j,1,len4}]//Flatten;
enhResult = InverseFourier[enhancTot];
(* Re-instate the correct abscissal scale and eliminate negative values of the ordinate. *)
distrScaled = Table[{data2[[j,1]], If[Re[enhResult[[j]] >= 0.0, Re[enhResult[[j]]], 0.0]}, {j, 1,
len4}];
graph5 = ListPlot[distrScaled, Plotjoined->True];
(* Show the non-resolution-enhanced and the enhanced data on the same graph. *)
Show[{graph2, graph5}];
```